

DEVELOPMENT AND VERIFICATION OF AN ALTERNATIVE FORMULATION FOR DYNAMIC REACTIVITY MEASUREMENT OF ROD WORTH

Imelda Ariani and Paul J. Turinsky

Electric Power Research Center
Department of Nuclear Engineering
North Carolina State University
P. O. Box 7909
Raleigh, NC 27695-7909
Email: iariani@eos.ncsu.edu and turinsky@eos.ncsu.edu

Doddy Y.F. Kastanya

Department of Nuclear Engineering
North Carolina State University
P.O. Box 7909
Raleigh, NC 27695-7909
Email: dfkastan@eos.ncsu.edu

Keywords: three-dimensional kinetic calculations, rod worth measurement, low-power physics testing

ABSTRACT

The measurement of control and shutdown rod worths are commonly required by the regulatory authorities as part of the start-up physics test program for Pressurized Water Reactors (PWR). In the early years of commercial nuclear power plant technology, the boron end-point method was employed. This option for measuring the rod worth can be very time consuming. In most cases, this method has been replaced by the rod swap method (RSM). The latest advancement in rod worth measurement technique is the dynamic reactivity measurement of rod worth (DRMRW). The DRMRW methodology is based on three dimensional, space-time kinetic simulations of rapid rod movement. This paper describes the methodology and experimental verification of the DRMRW technique that was developed by the North Carolina State University Electric Power Research Center (EPRC).

1. INTRODUCTION

Building upon the rod insertion method for rod worth measurement first introduced by the KRSKO nuclear power plant (Glumac and Skraba, 1989), Westinghouse (Chao, *et al.*, 1992 and 2000) developed their version of DRMRW referred to as dynamic rod worth measurement (DRWM^{TM 1}). EPRC has independently developed its version of the

1. DRWM is a registered trademark of Westinghouse Electric Company.

DRMRW methodology (Kastanya, 1997), implemented in the RAMBO computer code (EPRC, 1998). DRMRW experimental implementation follows that used for DRWMTM, that being to first establish the reactor critical with all banks out except a single bank which is slightly inserted. This bank is then withdrawn and a stable period is established. Immediately thereafter, the bank whose worth is to be measured is inserted at the maximum stepping rate. The excore detector signals and rod position are recorded as a function of time. From the excore detector signals, the measured static bank worth is determined *via* data processing utilizing core simulator predictions. Using DRMRW, the time needed to measure all bank worths can be reduced relative to the time required to complete RSM. In addition, the integral rod worth curves can be obtained.

2. METHODOLOGY

2.1. Overview

A flow diagram of the DRMRW methodology used to render the rod worth from the excore detector signals is presented in Fig. 1. After correcting the signals for background noise, the excore detector signals are utilized to determine the core-averaged flux. In this process, radial and axial flux spatial redistributions of the flux are corrected for. Given the core-averaged flux as a function of time, inverse point kinetics is then employed to determine the dynamic bank worth as a function of bank position, which is also recorded as a function of time. Since this is a dynamic experiment, the delayed neutron precursor number densities are not in equilibrium with the current flux level, implying that the rod worth obtained from inverse kinetics is the dynamic worth. The final step of the DRMRW is to convert the dynamic to static worth *via* dynamic to static correction factor (DSCF). The static worth can then be contrasted with the core simulator prediction of the rod worth.

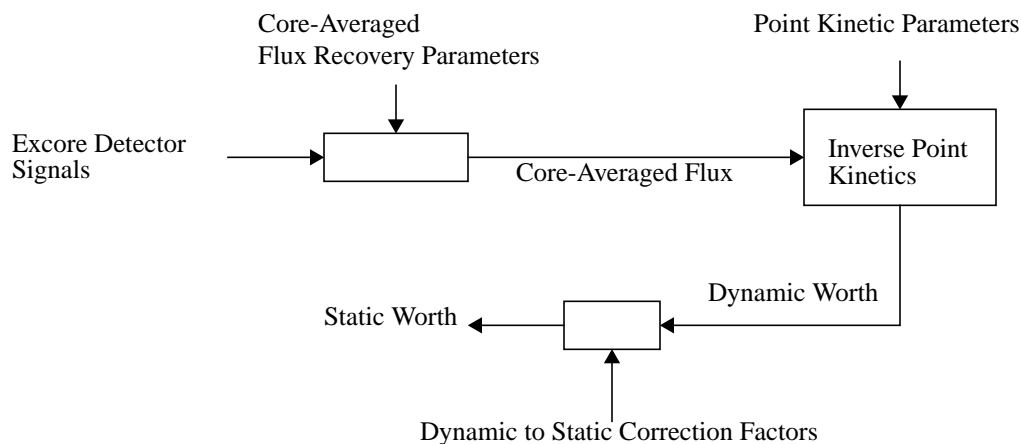


Fig. 1 Overall DRMRW Process.

2.2. Inverse Point Kinetics

The starting point of our discussion on the development of the DRMRW technique is the point kinetics equations whose associated neutron balance is given by

$$\frac{dn(t)}{dt} = \left(\frac{\rho(t) - \beta(t)}{l(t)} \right) n(t) + \sum_{i=1}^I \lambda_i(t) C_i(t), \quad (1)$$

and delayed neutron precursor balance equation is given by

$$\frac{dC_i(t)}{dt} = \frac{\beta_i(t)}{l(t)} n(t) - \lambda_i(t) C_i(t), \quad (2)$$

where:

$\rho(t)$ = core reactivity

$l(t)$ = prompt neutron generation time

$n(t)$ = core-averaged neutron density

$\lambda_i(t)$ = decay constant for precursor group i

$C_i(t)$ = core-averaged delayed neutron density for precursor group i

$\beta_i(t)$ = effective delayed neutron fraction for precursor group i

$\beta(t)$ = total effective delayed neutron fraction = $\sum_i \beta_i(t)$

The point kinetic parameter values are generated by the core simulator utilizing a variational technique derivation (Stacey, 1974). All point kinetic parameters are a function of time t through bank axial insertion position $r(t)$.

It will prove desirable to work in terms of the normalized core-averaged neutron density and precursor concentrations:

$$\bar{n}(t) \equiv n(t)/n(t_o) \text{ and } \bar{C}_i(t) \equiv C_i(t)/n(t_o), \quad (3)$$

where t_o denotes the time of initial bank insertion. Substituting Eq. (3) into Eqs. (1) and (2) produces Eqs. (4) and (5):

$$\frac{d\bar{n}(t)}{dt} = \left(\frac{\rho(t) - \beta(r(t))}{l(r(t))} \right) \bar{n}(t) + \sum_{i=1}^I \lambda_i(r(t)) \bar{C}_i(t) \quad (4)$$

$$\frac{d\bar{C}_i(t)}{dt} = \frac{\beta_i(r(t))}{l(r(t))} \bar{n}(t) - \lambda_i(t) \bar{C}_i(t). \quad (5)$$

The working equations involve two unknowns: the normalized core-averaged neutron density and precursor concentrations. It is desirable to solve Eq. (5) for the core-averaged precursor concentrations in terms of core-averaged neutron density. To accomplish this, first divide the time domain into discrete times $\{t_l\}$ and approximate the time dependence of the neutron density over time span $[t_{l-1}, t_l]$ by an exponential:

$$\bar{n}(t) = \bar{n}(t_{l-1}) \exp(\gamma_l(t - t_{l-1})) \quad (6)$$

where the exponential coefficient is determined by

$$\gamma_l = \frac{1}{\Delta t} \ln \left(\frac{\bar{n}(t)}{\bar{n}(t_{l-1})} \right). \quad (7)$$

Then, substitute Eqs. (6) and (7) into Eq. (5) and employ the integrating factor technique to express the precursor concentrations in terms of the neutron density at time t_l :

$$\bar{C}_i(t_l) = \bar{C}_i(t_{l-1}) e^{-\lambda_i(r(t_l))\Delta t_l} + \frac{\beta_i(r(t_l))}{l(r(t_l))} \left(\frac{\bar{n}(t_{l-1}) \left(e^{\gamma_l \Delta t_l} - e^{-\lambda_i(r(t_l))\Delta t_l} \right)}{\lambda_i(r(t_l)) + \gamma_l} \right), \quad (8)$$

where the time step size has been defined as $\Delta t_l \equiv t_l - t_{l-1}$ and all point kinetic parameters have been assumed constant over the time step at their new time values.

To utilize Eq. (8), the precursor concentrations at t_{l-1} must be known. This implies that the initial condition for the precursor concentrations must be known. The DRMRW experiment is initiated from a stable period. This implies that the precursor concentrations have the same behavior as the neutron density during a stable period. Utilizing this

behavior and the fact that by definition $\bar{n}(t_o) = 1$, one can provide the initial condition for the precursor concentrations:

$$\bar{C}_i(t_o) = \frac{\beta_i(r(t_o))}{l(r(t_o))} \left(\frac{1}{\lambda_i(r(t_o)) + \gamma_o} \right). \quad (9)$$

If the normalized core-averaged neutron density can be determined from the excore detector signals, one can solve for the precursor concentrations using Eq. (8). The detailed method of extracting core-averaged neutron density from the excore detector signals is given in section 2.3. The solved values of precursor concentrations, along with the core-averaged neutron density, can be used to determine the reactivity by rearranging Eq. (4):

$$\rho(t_l) = \beta(r(t_l)) + l(r(t_l)) \left(\gamma_l - \frac{1}{\bar{n}(t_l)} \sum_{i=1}^I \lambda_i(r(t_l)) \bar{C}_i(t_l) \right). \quad (10)$$

What is desired is the rod worth. Therefore, we must subtract off the positive core reactivity that exist during the stable period and reverse signs:

$$\text{Dynamic Rod Worth} = \Delta\rho^D(t_l) = -(\rho(t_l) - \rho(t_o)) \quad (11)$$

As noted previously, the rod worth determined from the inverse point kinetics is a dynamic worth since the spatial distributions of the neutron flux and precursor concentrations are not in equilibrium. Section 2.4. indicates how to obtain the measured static worth, where now the spatial distributions of the neutron flux and precursor concentrations are in equilibrium, from the measured dynamic worth.

2.3. Core-Averaged Flux Determination

To obtain the core-averaged flux from the excore detector signals, we need to account for both radial and axial spatial redistributions of the neutron flux during the experiment. If delayed neutrons are ignored, the relationship between the X detector signals (where X denotes top or bottom detector) and the flux distribution is given by

$$R^X(t_l) = \sum_n \Delta V_n w_n^X \sum_g v \Sigma_{g_n}(t_l) \phi_{g_n}(t_l), \quad (12)$$

where

ΔV_n = volume for spatial node n

w_n^X = X excore detector response factor for spatial node n

To determine the excore detector response factors, the response of the excore detector to the fission neutron source's energy and spatial dependencies must be determined. Since a typical core simulator only contains two energy groups (*i.e.* fast and thermal groups), additional energy detail is required. Let us introduce the excore detector response function, which is as function of fine neutron energy group and spatial position. The excore detector response factor can then be obtained by energy group collapsing the fine-group response function using the equilibrium neutron fission spectra at spatial node n . In practice, the response function is determined utilizing an S_n code such as DORT/TORT (RSIC Computer Collection, 1995) and solving for the generalized adjoint flux associated with the excore detector response.

The time and spatially dependent flux appearing in Eq. (12) is unknown and unobtainable from the experimental data; therefore, an approximation needs to be introduced to progress further. For that purpose, introduce the spatial redistribution function which is defined as:

$$f_{g_n}(t_l) = \phi_{g_n}(t_l)/\phi(t_l). \quad (13)$$

Since the absolute efficiency of an excore detector is unknown, all that we can determine are the relative excore detector signals. For this reason, introduce the normalized excore detector signal, defined as

$$\bar{R}^X(t_l) = R^X(t_l)/R^X(t_o), \quad (14)$$

which is not dependent upon the absolute excore detector efficiency if the efficiency assumed unchanged during the DRMRW. The total normalized excore detector signal is produced by combining the top and bottom normalized excore detector signals:

$$\bar{R}^{\text{total}}(t_l) = \bar{R}^{\text{top}}(t_l) + \bar{R}^{\text{bottom}}(t_l), \quad (15)$$

Using Eqs. (12), (13) and (14) in Eq. (15), and assuming the time dependence of cross-sections and spatial redistribution function can be approximated as only a function of rod position at steady-state conditions, we obtain

$$\bar{R}^{\text{total}}(t_l) = \bar{\alpha}^{\text{total}}(r(t_l))\bar{\phi}(t_l) \quad (16)$$

where the core-averaged flux to excore detector conversion factor (FRCF) is defined by

$$\bar{\alpha}^{\text{total}}(r(t_l)) = \frac{\Delta V_n w_n^X}{v \Sigma_{g_n}} r(t_l) \quad (17)$$

Solving Eq. (16) for the normalized core-averaged flux produces

$$\bar{\phi}(t_l) = \bar{R}^{\text{total}}(t_l) / \bar{\alpha}^{\text{total}}(r(t_l)). \quad (18)$$

where $\bar{R}^{\text{total}}(t_l)$ value is experimentally determined and $\bar{\alpha}^{\text{total}}(r(t_l))$ value is calculated. Utilizing the relationship between normalized core-averaged flux and normalized neutron density, one can determine the dynamic worth from the inverse point kinetics equations as described in section 2.2.

2.4. Dynamic to Static Correction Factor

As previously noted, the rod worth obtained from the inverse point kinetics equation is the dynamic rod worth. What we desire to contrast with is the core simulator prediction of the static rod worth. Therefore, a correction factor that will translate the dynamic worth into the static worth is needed. The dynamic to static correction factor (DSCF) is defined as:

$$\text{DSCF}(r(t)) = \frac{\text{Core Simulator Static Rod Worth}(r(t))}{\text{Simulated Dynamic Rod Worth}(r(t))}, \quad (19)$$

where $r(t)$ denotes the time-dependent rod position. A simulation sensitivity study revealed that the major dependencies of the DSCF are on bank type and bank (rod) axial position, with weak dependence on the rate of bank insertion, consistent with the characterization noted in Eq. (19). To obtain the DSCF values, it is necessary to complete a three-dimensional, space-time core simulation of the DRMRW experiment for each bank. From the DRMRW simulation, the time dependent fission neutron spatial distribution is obtained. Utilizing Eq. (12) the simulated top and bottom excore detector signals as a function of time are obtained. The simulated value of the dynamic rod worth can then be calculated using these simulated signals by processing them using the DRMRW methodology. Note that the DSCF is so defined that it not only converts the dynamic worth into the static worth, but also corrects for errors in the dynamic worth introduced by the approach used to obtain its value, such as the assumption that the spatial redistribution function appearing in (17) for the FRCF is only a function of rod position at steady-state conditions.

Finally, substituting the simulated dynamic rod worths and simulated static worths from steady state core simulator calculation into the right hand side of Eq. (19), the DSCF values are obtained. The measured static worth can then be obtained as follow:

$$\text{Measured static rod worth} = \text{DSCF}(r(t)) \times \Delta\rho^D(r(t)), \quad (20)$$

where $\Delta\rho^D(r(t))$ is calculated using Eq. (11).

3. EXPERIMENTAL VERIFICATION OF EPRC DRMRW METHODOLOGY

Duke Power has adopted Westinghouse's DRWMTM for their Westinghouse PWRs, implying that they have collected experimental data for a number of plants and reload cores. This provides the opportunity to utilize the EPRC RAMBO code (EPRC, 1998), which implements our DRMRW methodology, to reduce the experimental data collected by Duke Power and to contrast the resulting bank worths with those predicted using the Duke Power implementation of the DRWMTM methodology. The following section reports upon this experimental verification.

We currently have reduced experimental data for six reload cycles from three different plants, all plants being Westinghouse 4-loop NSSSs. The control and bank locations for the plants analyzed are shown in Fig. 2. In all cases, Duke utilizes the SIMULATE core simulator, using CASMO3 two-group provided cross-sections, to generate the DRWMTM pre-calculated parameters and predicted bank worths, and the Westinghouse DRWMTM methodology to determine the measured bank worth. By contrast, EPRC utilizes the NESTLE core simulator (Turinsky, 1994), using the same CASMO3 provided cross-sections, to generate the DRMRW pre-calculated parameters and predicted bank worths, and EPRC RAMBO code to determine the measured bank worths. These two approaches will be referred to as S-W (SIMULATE-Westinghouse) and EPRC for simplicity, recognizing that different core simulators are also involved. The information required to establish the reload cycle models for the NESTLE code and excor detector signals from the measurements were provided by Duke Power (Thomas, 2000). The top and bottom excor detector response functions were determined by EPRC utilizing the TORT S_n code.

		SA		CB		CC		CB		SA		
			SD		SB		SB		SC			
SA		CD				SE				CD		SA
		SC									SD	
	CB			CC		CA		CC				CB
		SB									SB	
	CC		SE	CA		CD		CA		SE		CC
		SB									SB	
	CB			CC		CA		CC				CB
		SD									SC	
SA		CD				SE				CD		SA
			SC		SB		SB		SD			
		SA		CB		CC		CB		SA		

Fig. 2 Control and Shutdown Bank Locations.

Table 1 contrasts the bank worths predicted by SIMULATE *versus* NESTLE core simulators. NESTLE predicted bank worths are slightly larger than SIMULATE predictions, but the agreements are very good. Note that in the tables the total bank worth is defined as the sum of the individual bank worths. The pcm and % differences of the measured bank worths determined using S-W and EPRC methodologies are presented in Table 2. For most cores and banks, individual bank measured worth differences are less than 3%, indicating a lack of sensitivity of measured bank worth to the core simulator and DRMRW methodologies being employed to reduce the experimental data. The largest % differences, but not largest pcm differences, consistently occurs for Shutdown Bank A (SA) for all cores, since it has the lowest worth bank in all cores. Table 3 shows the overall agreement between measured and predicted bank worths obtained using S-W and EPRC methodologies. Slightly better agreement between measured and predicted worths is noted for the EPRC methodology. Fig. 3 displays the measured and predicted bank worths obtained using the S-W and EPRC methodologies for the six reload cores analyzed, which correspond to a total of 54 measured banks. From this figure it can be seen that there does not appear to be any correlation between difference in measured and predicted bank worth and bank worth.

Table 1: Predicted bank worths.

	Core	SIMULATE					
		1	2	3	4	5	6
B A N K	CA	396.9	296.4	323.8	363.0	302.9	408.5
	CB	587.4	667.7	645.6	630.0	646.8	569.4
	CC	892.5	771.4	808.3	814.2	740.8	943.7
	CD	612.9	469.5	606.5	570.3	557.1	531.3
	SA	209.4	295.8	274.4	256.5	256.6	196.3
	SB	888.0	776.9	1045.1	929.5	998.9	826.1
	SC	428.0	437.5	483.2	436.9	443.8	387.8
	SD	424.3	442.9	484.2	444.3	443.4	388.3
	SE	500.1	506.4	500.7	509.3	521.7	469.0
	Total	4939.5	4664.5	5171.8	4954.0	4912.0	4720.4
		NESTLE					
	Core	1	2	3	4	5	6
B A N K	CA	400.9	293.7	322.7	368.7	302.7	409.5
	CB	592.2	681.0	656.4	628.3	652.1	576.2
	CC	897.8	778.9	818.3	825.5	747.7	954.0
	CD	619.1	473.7	603.2	573.9	567.4	533.3
	SA	213.2	303.0	275.8	256.1	261.9	198.5
	SB	889.0	788.2	1067.0	934.4	1042.8	835.3
	SC	432.9	444.1	485.6	438.3	451.6	390.1
	SD	430.1	448.3	486.4	444.0	451.4	390.5
	SE	501.	512.0	512.5	516.8	527.3	474.1
	Total	4976.5	4722.9	5227.9	4986.0	4969.0	4761.5

Note: worths shown are in pcm.

Table 2: Measured bank worth differences.

		EPRC - [S-W] (in pcm)						
		Core	1	2	3	4	5	6
B A N K	CA	-5.5	-7.4	-8.5	-7.4	-4.9	-5.2	
	CB	4.7	0.1	4.7	5.9	8.4	3.2	
	CC	4.7	-1.9	-2.3	1.1	5.6	4.0	
	CD	-28.1	-14.7	-13.1	-16.7	-7.7	-18.1	
	SA	-12.2	-17.9	-12.0	-14.3	-13.9	-9.3	
	SB	6.6	-2.6	10.1	14.2	23.7	10.1	
	SC	-9.7	-10.7	-8.7	-11.2	-5.9	-7.4	
	SD	-9.4	-10.3	-8.5	-10.5	-8.3	-6.6	
	SE	-5.6	-8.4	-8.1	-7.8	-2.0	-6.5	
	Total	-54.5	-73.8	-46.4	-46.7	-5.0	-35.8	
		% (EPRC - [S-W]) / [S-W]						
		Core	1	2	3	4	5	6
B A N K	CA	-1.49	-2.69	-2.90	-2.19	-1.69	-1.29	
	CB	0.75	0.01	0.71	0.87	1.27	0.53	
	CC	0.53	-0.24	-0.30	0.13	0.79	0.42	
	CD	-4.09	-3.17	-2.11	-2.81	-1.36	-3.33	
	SA	-5.20	-5.63	-3.96	-5.14	-5.34	-4.49	
	SB	0.75	-0.32	0.95	1.45	2.39	1.20	
	SC	-2.11	-2.40	-1.72	-2.43	-1.29	-1.83	
	SD	-2.05	-2.19	-1.67	-2.22	-1.84	-1.63	
	SE	-1.23	-1.65	-1.67	-1.56	-0.39	-1.45	
	Total	-1.08	-1.54	-0.89	-0.91	-0.10	-0.74	

Table 3: Measured versus predicted worth differences.

Bank	S-W		EPRC	
	RMS of pcm error ^a	RMS of % error ^b	RMS of pcm error ^a	RMS of % error ^b
CA	22.22	6.55	29.94	8.68
CB	36.11	5.81	34.83	5.60
CC	24.12	3.06	28.14	3.52
CD	33.22	5.49	20.10	3.54
SA	20.52	8.27	10.18	3.95
SB	27.89	3.18	27.48	3.02
SC	20.98	4.81	10.60	2.40
SD	24.60	5.62	13.91	3.14
SE	22.01	4.44	31.68	6.32
Total	107.37	2.21	57.76	1.15

$$\begin{aligned}
 \text{a: RMS} &= \sqrt{\left(\frac{1}{6}\right) \sum_{\text{core}=1}^6 (\text{Measured} - \text{Predicted})^2} \\
 \text{b: RMS} &= \sqrt{\left(\frac{1}{6}\right) \sum_{\text{core}=1}^6 \left(\frac{\text{Measured} - \text{Predicted}}{\text{Predicted}}\right)^2}
 \end{aligned}$$

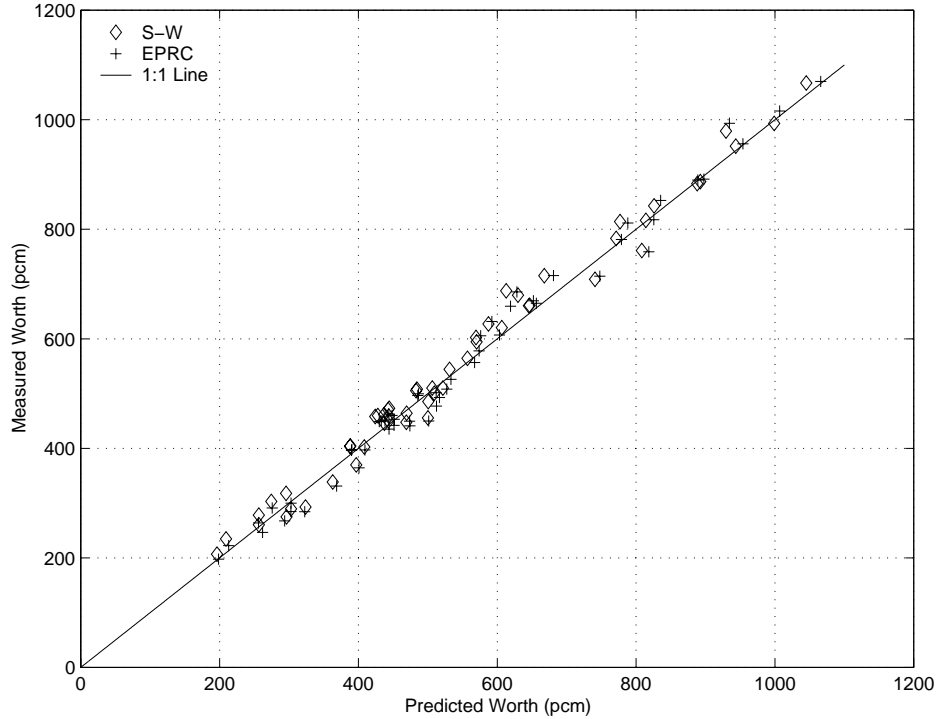


Fig. 3 DRMRW results summary.

4. CONCLUSIONS

The EPRC DRMRW methodology has been developed as an alternative method for determining rod worths. The overall procedure of the EPRC DRMRW technique was developed as follows. The excore detector signals were utilized to recover the core-averaged flux. The recovered core-averaged flux was then used with the inverse point kinetics equations to obtain the dynamic worth of the bank being measured. A correction factor, the dynamic to static correction factor which is assumed to be dependent upon only bank type and bank axial position, translates the measured dynamic worth into the measured static worth. As the final step, the measured static worth would then be compared to the steady state bank worth predicted using a core simulator code as a part of the acceptance criteria. The EPRC DRMRW methodology has been verified utilizing Duke Power's experiment data. The DRMRW results obtained using the EPRC methodology are in good agreement with the results obtained using the S-W methodology.

REFERENCES

Chao, Y.A., Chapman, D.M. Easter, M.E. Hill, D.J., Hoerer, J.A., 1992. Methodology of the Westinghouse Dynamic Rod Worth Measurement Technique. *Trans. Am. Nucl. Soc.*, **66**, 479.

Chao, Y.A, Chapman, D.M., Hill, D.J., Grobmyer, L.R., 2000. Dynamic Rod Worth Measurement. *Nucl. Tech.*, **132**, 403.

EPRC. RAMBO Version 1.0.0 Users Manual, Electric Power Research Center, North Carolina State University, 1998.

Glumac, B., Skraba, G., 1989. Rod Insertion Method for Rod Worth Measurement. *Proc. Technical Committee Mtg. Operational Safety of Two-Loop Pressurized Water Reactors*, IAEA/TC-650

Kastanya, D.Y.F., 1997. Development and Verification of the Dynamic Rod Worth Measurement Technique. Master of Nuclear Engineering Project Report, North Carolina State University.

RSIC Computer Code Collection. TORT-DORT: Two- and Three- Dimensional Discrete Ordinates Transport Version 2.12.14, Radiation Shielding Information Center, Oak Ridge National Laboratory, 1995.

Stacey, W.M., 1974. *Variational Methods in Nuclear Reactor Physics*, Academic Press.

Thomas, S.B. Duke Power Company, Private Communication, 2000.

Turinsky, P.J., Al-Chalabi, R.M., Engrand, P., Sarsour, H.N., Faure, F.X., Guo W. NESTLE, A Few-Group Neutron Diffusion Equation Solver Utilizing the Nodal Expansion Method for Eigenvalue, Adjoint, Fixed-Source, and Transient Problem, Idaho National Energy Laboratory, 1994.